College of Saint Benedict and Saint John's University

DigitalCommons@CSB/SJU

Effects of Oxidation on Protein-Nanoparticle Interactions

Valdez R. Rahming
College of Saint Benedict/Saint John's University

Md. Abul Fazal
College of Saint Benedict/Saint John's University, mfazal@csbsju.edu

Recommended Citation

Effects of Oxidation on Protein-Nanoparticle Interactions

Valdez R. Rahming[1] and Md. Abul Fazal[1*]

[1]*Department of Chemistry, College of Saint Benedict, 37 South College Avenue, Saint Joseph, MN 56374, U.S.A.*

Authors' contributions

This work was carried out in collaboration between the two authors. Author MAF designed the study, wrote protocol, managed the analyses of the study and wrote the manuscript. Author VRR performed the experiments, managed the analysis and literature searches. All authors read and approved the final manuscript.

Original Research Article	

ABSTRACT

Aims: Upon entrance into the blood stream most nanoparticles bind to an array of proteins forming a "protein corona". Fibrinogen is the second most abundant blood protein and has been reported to bind to a variety of nanoparticles including metal oxides, polymeric nanoparticles and carbon nanotubes.

Study Design: Study the effects of oxidation on the binding interactions between human serum fibrinogen and magnetic iron (III) oxide nanoparticles.

Place and Duration of Study: Department of Chemistry, College of St. Benedict, 37 South College Avenue, St. Joseph, MN 56374, U.S.A., between June 2011 and May 2012.

Methodology: Spectroscopic techniques (UV-Vis, IR, fluorescence, and circular dichroism) were used to study the binding interactions of magnetic nanoparticles with human serum fibrinogen and the effects of protein oxidation on its binding affinity.

Results: Magnetic nanoparticles (MNP) formed stable complex with fibrinogen under physiological conditions. The binding constants (K_a) were determined as 1.91 (± 0.14) $\times 10^6$ M^{-1} and 1.06 (± 0.09) $\times 10^6$ M^{-1} at 300 K and 310 K respectively. The secondary structure of the protein was slightly affected by the formation of fibrinogen-MNP complex. When the protein was oxidized with metal catalyzed oxidation (MCO) system, significant changes in the protein structure was detected leading to decreased binding affinity for

---

*Corresponding author: Email: mfazal@csbsju.edu;

MNP.
Conclusion: Metal catalyzed oxidation of fibrinogen significantly affects its binding interactions with magnetic iron (III) oxide nanoparticles.

1. INTRODUCTION

Nanoparticles (1-100 nm) are potentially useful tools in medicine and biology as they are of comparable size to important biological components (e.g. DNA, proteins, cell membranes) with which they interact [1]. Over the last two decades, numerous potential applications of nanoparticles have been reported in biomedical imaging, biosensing, drug delivery, and electronic devices [2]. Recently, the interaction of nanoparticles with proteins has emerged as a key area of study [3]. Most nanoparticles, upon contact with biological matrices, are immediately coated by proteins leading to the formation of a protein corona that largely defines the biological identity of the particle. This protein-nanoparticle interaction may alter protein conformation, expose new epitopes on the protein surface or perturb the normal protein function [4]. Adsorption onto nanoparticles has been found to induce protein aggregation, misfolding, and deactivation [5]. Because the adsorbed proteins determine the route of internalization, organ disposition and rate of clearance from bloodstream, the protein-nanoparticle interactions are important for understanding biodistribution, biocompatibility and therapeutic efficacy of nanoparticles. Currently, the mechanism of protein binding to nanoparticles is not well characterized.

Due to their unique magnetic properties, magnetic iron (III) oxide nanoparticles (MNP) have been used for a wide range of biomedical applications such as targeted delivery of drugs and genes, contrast-enhancing agent for magnetic resonance imaging (MRI), cell engineering, tissue repair, and hypothermia [6]. Magnetic nanoparticles have also been reported for many *in vivo* applications including acting as a tracer of blood flow and inducing clotting in arteriovenous malformations [7]. Upon administration of MNP intravenously, they immediately interact with common human plasma proteins, including human serum albumin, fibrinogen, apolipoprotein A-1, and immunoglobulin G. Initially abundant proteins dominate the surface of nanoparticles before they are displaced by less abundant proteins with higher affinity and slower interaction kinetics. Previous kinetic studies on solid lipid nanoparticles showed that initial protein binding was dominated by albumin, which was replaced over time by fibrinogen followed by apolipoproteins [8].

Fibrinogen is an adhesive protein that plays a pivotal role in hemostasis [9]. In response to blood vessel injury, platelets aggregate along with fibrin clots and adhere to extracellular matrix components readily exposed at the site of vascular damage [10]. Fibrinogen is the second most abundant protein in human serum. Studies showed that fibrinogen is the most easily oxidized protein in human blood [11]. Recently the interactions of fibrinogen with gold nanoparticles, titanium oxide and polystyrene nanoparticles have been reported [12-14].

Reactive oxygen species (ROS) and free radicals contribute to a state of "oxidative stress" when the cellular antioxidant systems cannot completely inactivate the ROS (O_2^-, $OH^.$, H_2O_2, singlet oxygen) arising from excessive production of ROS, loss of antioxidant defenses, or both. Increases in ROS damage proteins, nucleic acids, membrane lipids, and carbohydrates and can severely compromise cell health and viability leading to cell death.

Persistent oxidative stress has been implicated in various pathological conditions involving cardiovascular disease, cancer, diabetics, ischemia/reperfusion, and neurodegenerative diseases [15].ROS modification leads to increased levels of oxidized amino acid side chains, carbonylation and glycation [16]. Proteins are also known to be modified by lipid oxidation products such as malondialdehyde (MDA) and 4-hydroxy-2-nonenal (HNE) [17]. Oxidative modifications in albumin, the most abundant plasma protein, have been linked to reduced binding for Cu^{2+} ions [18]. Oxidation of fibrinogen results in decreased binding activity to platelet receptor GpIIb/IIIa and delayed fibrin lysis via plasminogen and tissue plasminogen activator [19-20].

In this study, human serum fibrinogen (HSF) was taken as a model protein to investigate the effects of oxidative modifications on its binding interactions with magnetic iron (III) oxide nanoparticles using spectroscopic methods. This paper reports binding constants, quenching mechanisms, and conformational changes for fibrinogen-MNP interactions under normal and oxidative stress conditions.

2. MATERIALS AND METHODS

2.1 Chemicals and Reagents

Phosphate buffered saline (PBS), human serum fibrinogen (50-70%) (HSF), magnetic iron (III) oxide nanoparticles (~ 10 nm) solution, and L-ascorbic acid sodium salt (99%) were purchased from Sigma and used as received. Ammonium carbonate and ethanol (absolute) from Sigma-Aldrich, coomassie Blue G-250 and guanidine hydrochloride from Research Organics, ethylenediaminetetraacetic acid (EDTA) and trichloroacetic acid from Fisher Scientific were also used (reagent grade).

2.2 UV-Vis Spectrophotometry

Separate solutions comprised of 0.87 μM HSF, 0.22 μM MNP, and a single solution containing both 0.87 μM and 0.22 μM HSF and MNP respectively were prepared in 0.01M PBS buffered to a pH of 7.4. A Cary-50 Bio UV- Visible Spectrometer and a 10 mm path length quartz cuvette were used to obtain absorbance measurements (200-500 nm). The expected absorption spectrum of HSF- MNP complex was obtained by mathematically adding the individual spectrum of HSF and MNP. To assess the stability of HSF-MNP complex over time, a solution containing 0.018 μM HSF and 0.14 μM MNP was prepared (0.01M PBS) and absorbance at 280 nm were recorded at five minutes intervals for three and half hours [21]. A 0.01M PBS solution was used as a blank for all measurements.

2.3 Fluorescence Spectroscopy

All fluorescence quenching studies were performed using an OLIS DM45 spectrofluorimeter and a 10 mm cuvette. For each titration of HSF (both oxidized and unoxidized) against MNP,solutions containing the same concentration of HSF along with increasing MNP concentrations were prepared in 0.01M PBS buffered to a pH of 7.4 . The emission spectra were recorded between 300 and 390 nm after excitation at 283 nm. This procedure was performed at temperatures of 300 K and 310 K for the protein samples.

2.4 Circular Dichroism (CD) Spectroscopy

The CD spectra were obtained using a JASCO-810 spectropolarimeter equipped with a thermostatically controlled cell holder. The temperature of the samples was controlled at 25 ± 0.1 ^{0}C. A 1 mm path length cuvette was used for all measurement. The CD spectra were generated by scanning between 200 and 320 nm with an average of three scans and a band width of 5 nm. The final spectra were obtained by subtracting the buffer contribution from the original protein spectra.

2.5 Oxidation of Fibrinogen

HSF was oxidized according to the procedure outlined by Tetik, Sermin, et al [19]. A 0.42 μM HSF solution was introduced to a Fe^{3+}/ascorbate oxidation system with a final concentration of 100 μM and incubated at a constant temperature of 37 ^{0}C using a water bath. Aliquots were taken after 0, 4, 8, 12, and 24 hours of incubation and quenched by the addition of the metal chelating agent EDTA at a final concentration of 1 mM. The oxidized samples were then dialyzed at 4°C using Spectra/Por MWCO dialysis membranes (MWCO: 12-14 kDa) and filtered via buchner filtration system.

2.6 Carbonyl and Protein Concentration Determination

Carbonyl concentrations for the control and oxidized samples were determined according to the procedure outlined by C.L. Hawkins et al. [22]. A control solution was prepared without the addition of the Fe^{3+}/ascorbate oxidation system in order to determine the effect of incubation on the protein samples. The Bradford assay (absorbance at 595nm) was used to determine the concentration of HSF after the oxidation procedure in order to account for any protein that was lost during the oxidation process.

2.7 Data Analysis

All experimental parameters were estimated as an average of three individual experiments and expressed as mean ± standard deviation (n = 3). Where necessary, statistical analyses were performed using student's t test.

3. RESULTS AND DISCUSSION

3.1 Fibrinogen-magnetic Nanoparticles Binding Interactions

UV-Vis absorption is a simple and applicable method to explore complex formation [23]. As shown in Fig. 1a, fibrinogen has two strong absorption bands at 230 nm and 280 nm. The 230 nm band is mainly due to the transition of $\pi \rightarrow \pi^*$ of fibrinogen's characteristic polypeptide backbone structure C=O [24]. Fig. 1b represents the absorption spectrum of MNP only. When MNP were added, the UV-Vis spectrum (Fig. 1d) was discernibly different from the sum of the absorbance of fibrinogen and MNP (Fig. 1c). The conformational changes reflected by spectral difference at 230 nm in the UV-Vis spectra might arise from disturbances of polypeptide's environment of the fibrinogen [25]. The stability of fibrinogen-MNP complex was examined by monitoring absorbance at 280 nm over time. No significant changes in absorbance was detected over the length of study (three and half hours) suggesting a very stable complex formation (data not shown).
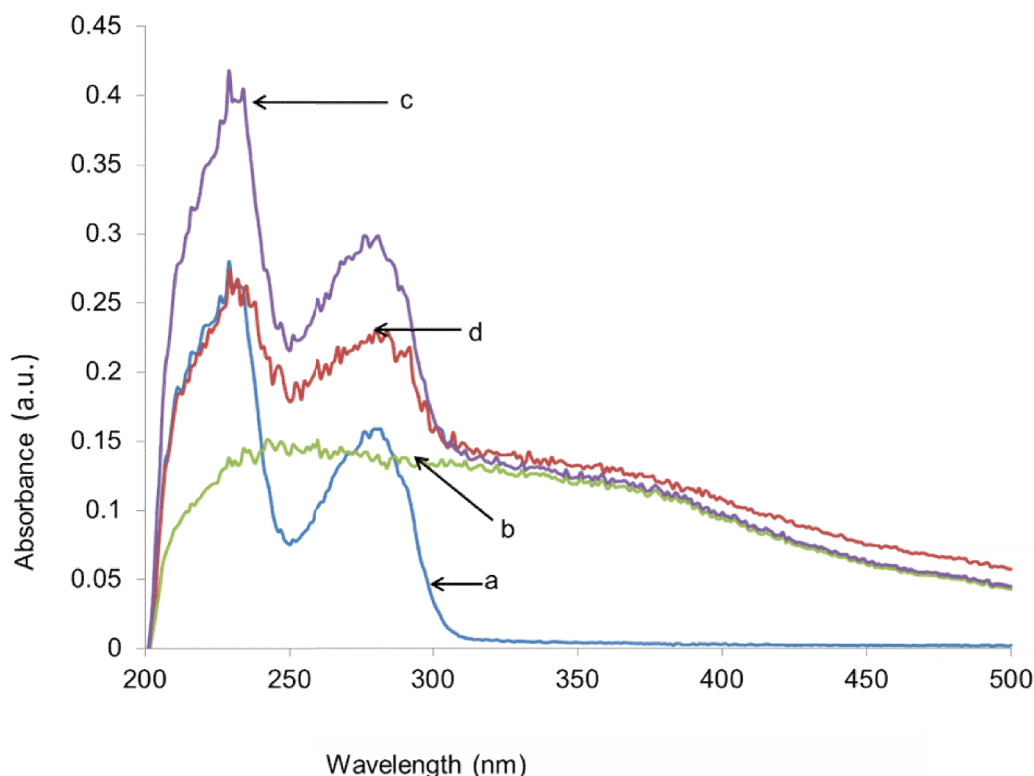
Fig. 1. UV-Vis absorption spectra of fibrinogen and fibrinogen-MNP complex
(a) A 8.7 x 10^{-7} M fibrinogen solution only, (b) A 2.2 x 10^{-7} M MNP solution only, (c) mathematical sum of the absorption spectra of fibrinogen (a) and MNP (b), and (d) fibrinogen-MNP complex with a concentration of 8.7 x 10^{-7} M fibrinogen and 2.2 x 10^{-7} M MNP. All solutions were made in 0.01 M PBS buffered to a pH of 7.4.

The binding interactions of fibrinogen and MNP were studied with spectrofluorimetry. A fixed concentration of fibrinogen in PBS was titrated with increasing concentrations of MNP. The protein was excited at 283 nm and the fluorescence signal was collected for 300 nm – 400 nm with an emission maximum of 338 nm. As shown in Fig. 2, the fluorescence intensity of the system decreased progressively with increased MNP concentrations. No obvious wavelength shift in emission maximum was observed for the MNP concentration range. Fluorescence results were used to determine the binding constant (K_a) using the equation shown below [26]:

$$log \frac{F_0 - F}{F} = logKa + nlog[Q] \qquad (1)$$

whereK_a is the binding constant (the reciprocal of K_d), n is the number of binding sites per HSF, [Q] the concentration of MNP, and F and $F_o$represent the fluorescence intensities of HSF in the presence and absence of MNP respectively. The values of K_a were obtained from the antilog of the y-intercept of the double logarithm regression curve log $(F_0 - F)/F$ versus log [Q] (Fig. 3). The binding constants were 1.91 (± 0.14) x 10^6 M^{-1} and 1.06 (± 0.09) x 10^6 M^{-1} at 300 K and 310 K respectively (n = 3). The linear correlation coefficients of the plots were larger than 0.99 indicating that the interactions between protein and MNP agreed well

with the site binding model in equation 1. Similar binding constants have been reported for many protein-nanoparticle interactions including fibrinogen. Lacerda et al. studied the interactions of gold nanoparticles with common human blood proteins and reported the binding constant of human serum fibrinogen with 10 nm gold particles as 0.65×10^6 M^{-1} [27]. Yang et al. reported the binding constant of bovine serum albumin with 10 nm iron oxide nanoparticles as 2.40×10^6 M^{-1} [28].
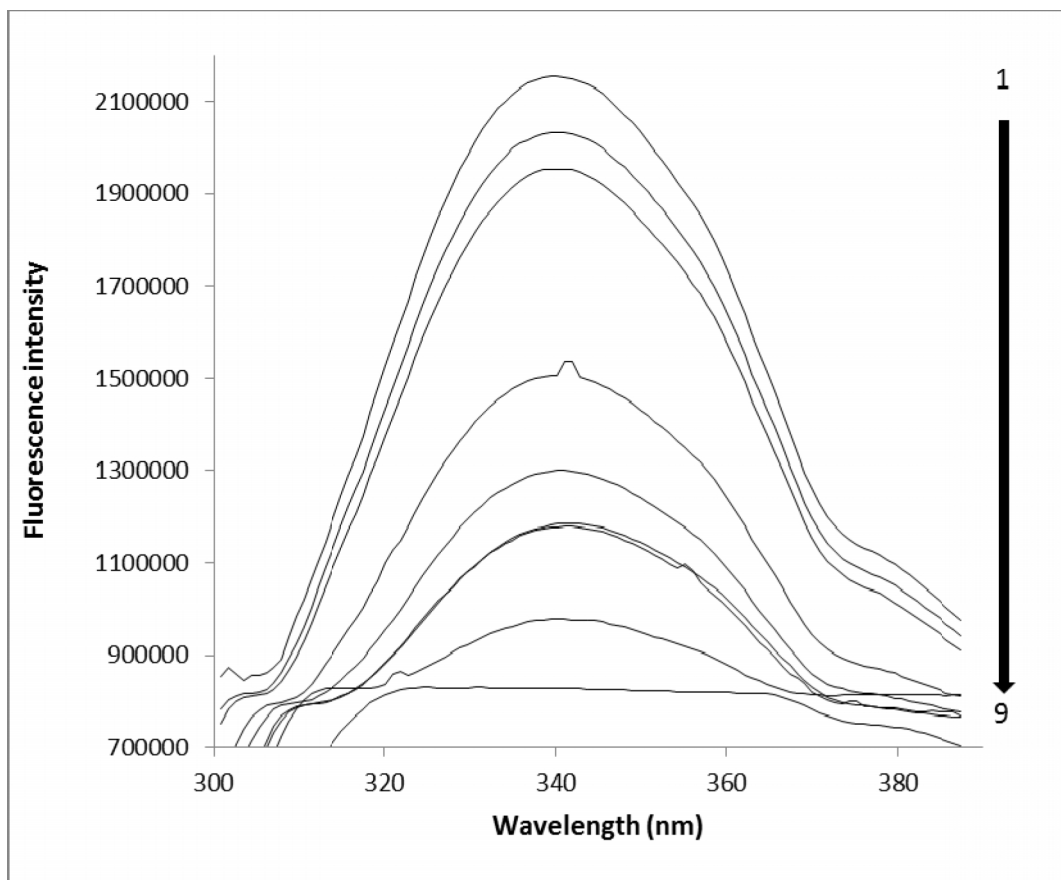

Fig. 2. Fluorescence spectra of fibrinogen in the presence and absence of MNP.
Fibrinogen concentration was fixed at 1.0×10^{-6} M. MNP concentrations were (1) 0, (2) 0.4, (3) 0.8, (4) 1.2, (5) 1.6, (6) 2.0, (7) 2.4, (8) 2.8, and (9) 3.2 ($x~10^{-6}$ M) respectively. The fluorescence spectra were obtained by exciting at 283 nm.
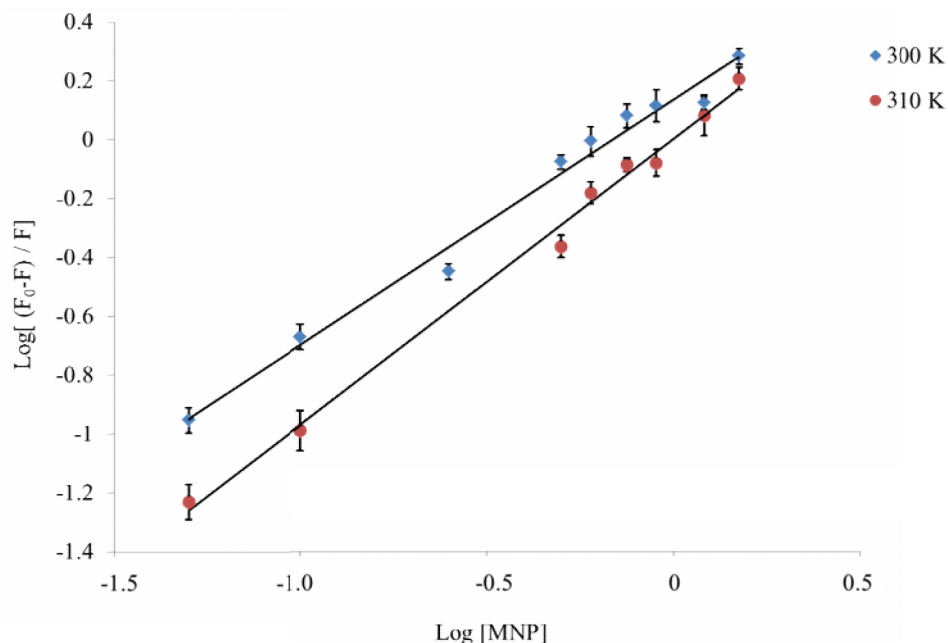
Fig. 3. Double-log plot of MNP quenching effect on fibrinogen fluorescence at 300 and 310 K (n = 3).

3.2 Quenching Mechanism Analysis

Fluorescence quenching is the decrease of quantum yield of fluorescence from a fluorophore induced by a variety of molecular interactions including excited-state reactions, molecular rearrangements, energy transfer, ground-state complex formation and collisional quenching [29]. These different quenching processes can be divided into two broad categories i.e. dynamic quenching and static quenching. Dynamic quenching is caused by collisions between the quencher and the fluorophore during the lifetime of excited state whereas static quenching refers to fluorophore-quencher complex formation. Fluorescence quenching can be described by the Stern-Volmer equation [30]:

$$\frac{F_0}{F} = 1 + K_{SV}[Q] = 1 + K_q\tau_0[Q] \qquad (2)$$

where F_0 and F represent the fluorescence intensities in the absence and presence of quencher respectively, K_{sv} is the dynamic quenching constant, K_q is the quenching rate constant, $[Q]$ is the concentration of quencher and τ_0 is the average fluorescent life time of the molecule without quencher.

Dynamic and static quenching can be distinguished by their different dependences on temperature. Dynamic quenching is caused by a collision which means that higher temperatures will result in larger diffusion coefficients. As a result, the quenching constants (K_{sv}) are expected to increase with temperature. In contrast, static quenching is dominant when increased temperature results in decreased K_{sv} of the quenching. The dynamic quenching constants (K_{sv}) calculated for fibrinogen-MNP complexes at two different temperatures 300 and 310 K were 1.60 ($\pm$ 0.02) x 10^6 M^{-1} and 1.02 ($\pm$ 0.03) x 10^6 M^{-1}

respectively (Fig. 4). The dynamic quenching constant decreased by about 38% for 10 degrees increase in temperature. The quenching rate constants, K_q were calculated from the K_{sv} values (the τ_0 for the biopolymer is often taken as 10^{-8} s) [31]. The calculated values of K_q were 1.56 ($\pm$ 0.06) x 10^{14} and 1.12 ($\pm$0.04) x 10^{14} L.mol^{-1}s^{-1} at 300 K and 310 K respectively.
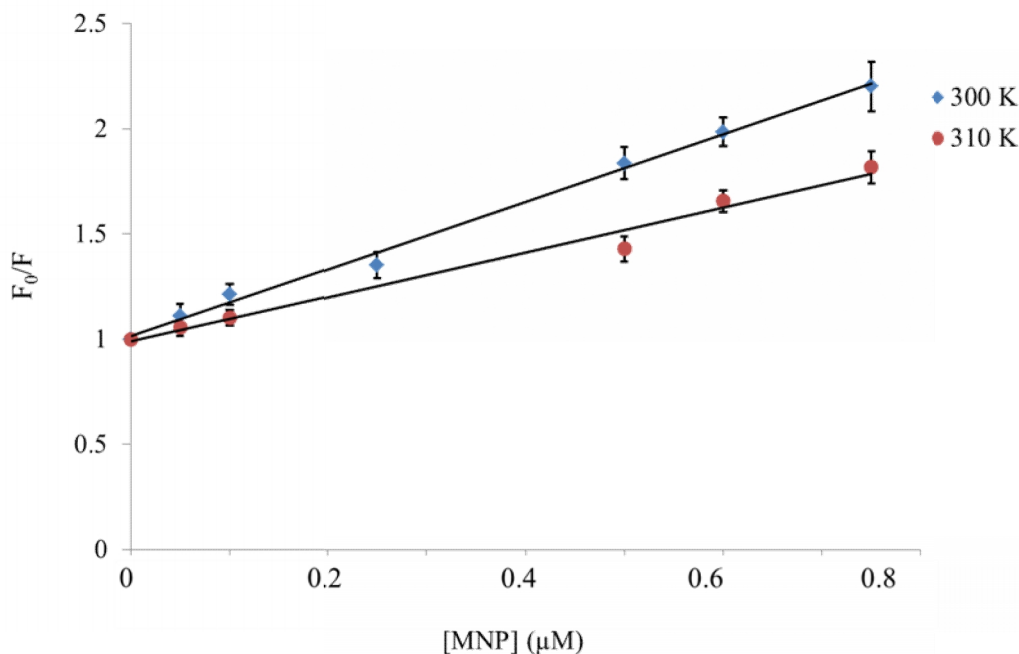

Fig. 4. Stern-Volmer plots of F_0/F vs. concentration of MNP at 300 and 310 K (n = 3).

According to the literature, for dynamic quenching, the maximum collision-quenching rate constant (K_q) of various quenchers with the biopolymer is 2.0 x 10^{10} L.mol^{-1}s^{-1} [32]. Considering that the quenching rate constant for fibrinogen-MNP interaction is much greater than 2.0 x 10^{10} L.mol^{-1}s^{-1} and that the K_{sv} decreased with increased temperature, it can be concluded that the quenching is initiated probably by static quenching resulting from the formation of fibrinogen-MNP complexes. Static quenching has also been reported for bovine serum albumin complexes with Ag(I) and magnetic iron (III) oxide nanoparticles [28,33].

3.3 Conformational Analysis

Circular dichroism (CD) spectroscopy is a quantitative technique to investigate the conformation of proteins and peptides in aqueous solutions [34]. CD spectroscopy was performed to investigate any changes in the secondary and tertiary structure of fibrinogen due to binding with MNP (Fig. 5). The far-UV CD spectrum (205 nm – 250 nm) of fibrinogen exhibits two negative peaks at 208 nm and 222 nm which reflect the characteristics of α-helices [35]. The two peaks are attributed to the n→π* transition for the peptide bond of α-helix. The α-helix contents of free and bound fibrinogen were calculated at 208 nm using the equation [36]:

$$\alpha - helix(\%) = -\frac{[MRE_{208} - 4000]}{[33000 - 4000]} \times 100 \qquad (3)$$

where, MRE_{208} is the observed mean residue ellipticity (MRE) at 208 nm, 4000 is the MRE of the β form and 33000 is the MRE value of pure α-helix at 208 nm.

The α-helix content of free fibrinogen was estimated to be ~31% which is close to the literature value of 32% to 37% in PBS [37]. The addition of MNP caused a slight reduction of α-helix content to 29.83% which indicated that MNP bound to the amino acid residues of the main polypeptide chain of fibrinogen and may have interfered with the hydrogen-bond networks in the region of contact. No noticeable shift in the ellipticity of fibrinogen in the near-UV region (250-320 nm) was observed after binding with MNP (data not shown). These findings are consistent with literature showing mild or no changes in α-helix content of fibrinogen after binding with nanoparticles [38-39].
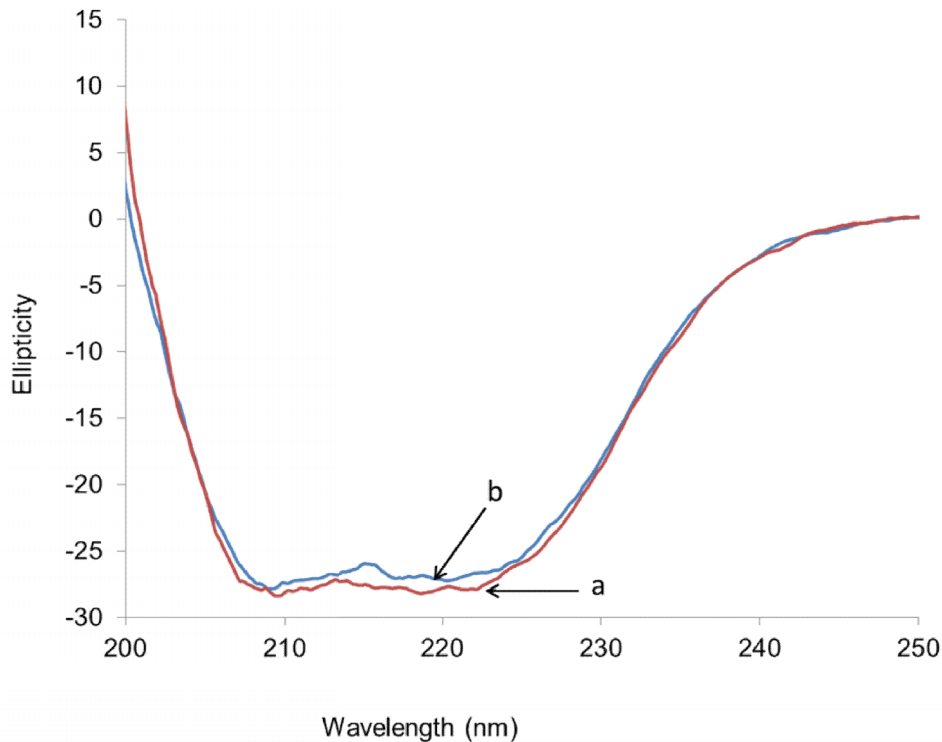

Fig. 5. Far-UV CD spectra of fibrinogen in absence (a) and presence (b) of MNP
The concentrations of HSF and MNP were 9.0 x 10^{-7} M and 6.0 X 10^{-7} M respectively in 0.01 M PBS buffer at pH = 7.4. The CD spectra were collected at 25 ^{0}C with an average of three scans.

3.4 Effect of Oxidation on Fibrinogen-MNP Interactions

To investigate the effect of oxidative modifications of protein on protein-MNP binding interactions, fibrinogen was oxidized using a metal-catalyzed oxidation (MCO) system [19]. The oxidation of protein usually results in formation of carbonylated amino acid residues. Therefore, the formation of such groups was measured as a function of time. Fig. 6 shows a clearly detectable increase in the amount of fibrinogen-bound carbonyl groups. Formation of carbonyl groups did not reach plateau after 24 hours but incubation for longer than 24 hours resulted in the development of turbidity indicating the denaturation of the protein.
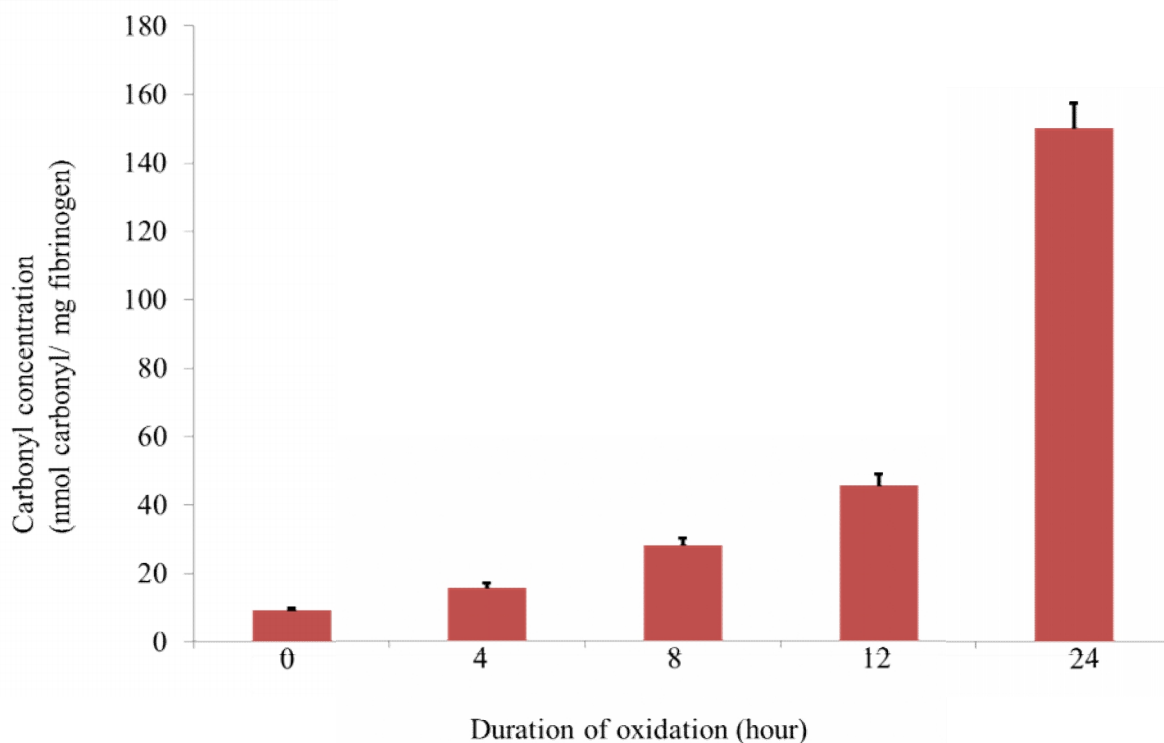
Fig. 6. Carbonyl concentration of oxidized fibrinogen as a function of time
A 0.42 µM HSF solution was incubated with 100 µM metal catalyzed oxidation (MCO) system at 37 ^{0}C. Carbonyl groups were measured as DNPH hydrazine derivatives and expressed as nmol carbonyl / mg protein (n = 3).

Steady state fluorescence measurements were used to determine the binding constant for oxidized fibrinogen and MNP. The results are summarized in Fig. 7. Oxidation of fibrinogen caused a significant decrease in binding constants. After 4 hours of oxidation, fibrinogen showed a 75% loss in binding constant compared to that of unoxidized protein. Further oxidation of fibrinogen (8, 12, and 24 hours) resulted in insignificant binding. Anraku et al. studied the effects of oxidative stress on the structure of human serum albumin using a metal catalyzed oxidation system and concluded that the oxidation process affected the secondary structure of albumin but did not denature the protein [40]. The conformational changes of albumin resulted in a more open protein molecule with a higher degree of exposure of hydrophobic area. Petronio et al. studied the effects of oxidation of bovine serum albumin by HOCl and HOBr and showed that the α-helix content of BSA reduced from 49.5% to 42.4% after treatment with HOBr [41]. The structural properties of oxidized fibrinogen were examined by CD spectroscopy. The MCO mediated oxidation caused a gradual loss of in α-helix (data not shown). The α-helix contents in fibrinogen after 4, 8, 12, and 24 hours of oxidation were calculated to be 28.60%, 27.20%, 24.52% and 16.24% respectively. The effect of oxidation on fibrinogen was also monitored by measuring dityrosine formation. Tyrosine residues are known to form dityrosine under oxidative stress conditions [42]. The status of tyrosine was examined by fluorescence measurement of dityrosine (excitation λ_{max} = 320 nm, emission λ_{max} = 410 nm). After 4 hours of oxidation, fibrinogen showed a 20% increase in dityrosine fluorescence compared to the unoxidized

protein. These findings indicate that MCO mediated oxidation significantly affected the secondary structure of fibrinogen and led to decreased binding with magnetic nanoparticles.
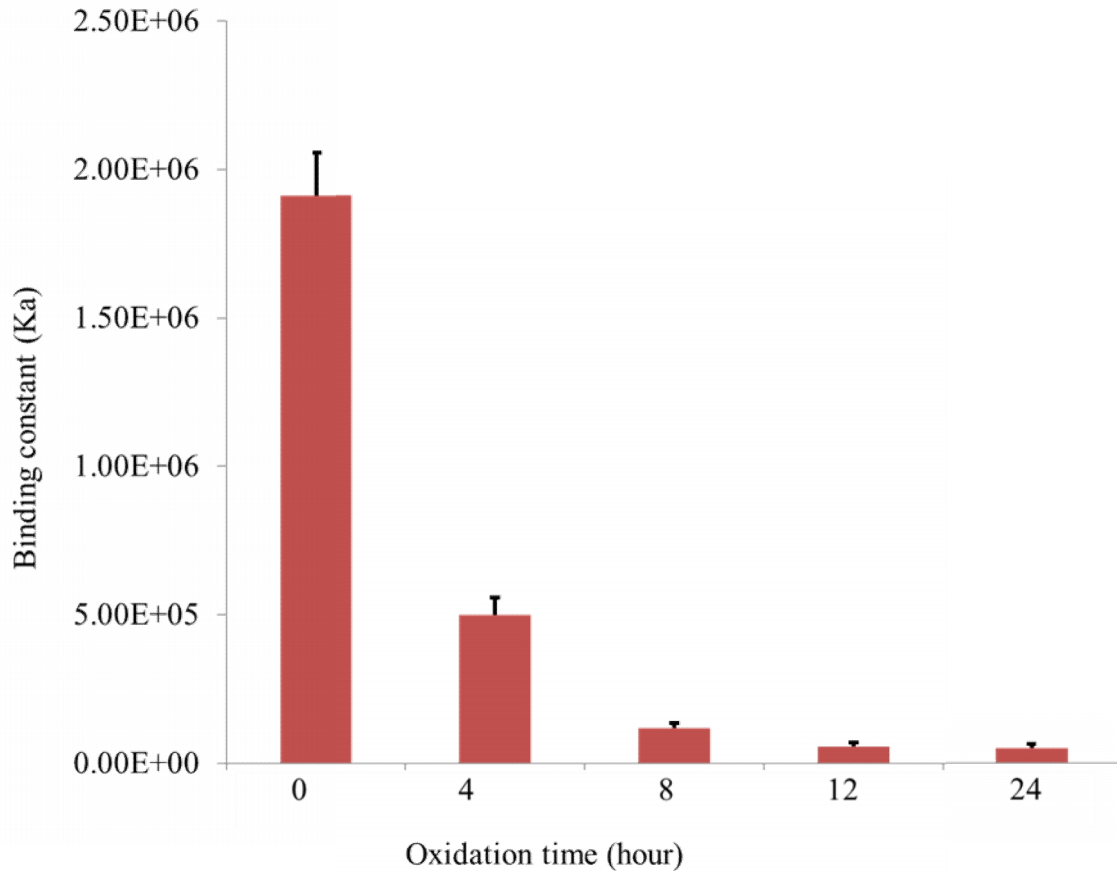

Fig. 7. Binding constant (K_a) of fibrinogen and MNP as a function of oxidation time (n = 3).

4. CONCLUSION

This study was designed to investigate the nature and magnitude of fibrinogen-MNP binding interactions and the effects of oxidative modifications of fibrinogen on binding. The results showed that fibrinogen formed a stable complex with MNP under physiological conditions. In the process of binding, MNP caused a decrease in the intrinsic fluorescence of fibrinogen through the static quenching mechanism. Metal catalyzed oxidation of fibrinogen resulted in significant changes in the structure of the protein and adversely affected its binding affinity with magnetic nanoparticles. These findings are important because fibrinogen is known as an adhesive plasma protein that plays a pivotal role in hemostasis and its oxidation by reactive oxygen species (ROS) could affect the blood coagulation process. However, given the comparatively high fibrinogen concentration in blood, the effect of physiological ROS on fibrinogen oxidation could be minimal.

CONSENT

Not applicable.

ETHICAL APPROVAL

Not applicable.

ACKNOWLEDGEMENTS

COMPETING INTERESTS

Authors have declared that no competing interests exist.

REFERENCES

1. Banard AS. Nanohazards: knowledge is our first defence. Nature Materials. 2006**;**5:245-248.
2. Moghimi SM, Szebeni J. Stealth liposomes and long circulating nanoparticles: critical issues in pharmacokinetics, opsonization and protein binding properties. Prog. Lipid Res. 2003;42:463-478.
3. Lundqvist M, StiglerJ, EliaG, LynchI, CedervallT, Kenneth A, Dawson K. Nanoparticle size and surface properties determine the protein corona with possible implications for biological impacts. Proc. Natl. Acad Sci. U.S.A. 2008;105:14265-14270.
4. Lynch I, Dawson KA, Linse S. Detecting cryptic epitopes created by nanoparticles. Sci. STKE. 2006; pe 14.
5. Zhang D, Neumann O, Wang H, Yuwono VM, Barhoumi A, Perham M, Hartgerunk JD, Wittung Stafshede P, Halas NJ. Gold nanoparticles can induce the formation of protein- based aggregates at physiological pH. Nano Lett. 2009;9:666-671.
6. Sing N, Jenkins GJS, Asadi R, Doak SH. Potential toxicity of superparamagnetic nanoparticles (SPION). Nano Reviews. 2010;1:5358.
7. Gupta AK, Gupta M. Synthesis and surface engineering of iron oxide nanoparticles for biomedical applications. Biomaterials. 2005;26:3995-4021.
8. Goppert TM, Muller RH. Adsorption kinetics of plasma proteins on solid lipid nanoparticles for drug targeting. International Journal of Pharmaceutics. 2005;302:172-186.
9. Esmon CT. The protein C pathway. Chest. 2003;124:26s-32s.
10. Ulutin ON. Atherosclerosis and hemostasis. Semin Thromb Hemost. 1986;12(2):156-174.
11. Upchurch GR, Ramdev N, Walsh MT, Loscalzo J. Prothrombotic consequences of the oxidation of fibrinogen and their inhibition by aspiration. J. Thromb Thromblysis. 1998;5(1): 9-14.

12. Deng ZJ, Liang M, Toth I, Monteiro MJ, Minchin RF. Molecular interactions of poly(acrylic acid) gold nanoparticles with human fibrinogen. ACS NANO. 2012;6(10):8962-8969.

13. Wang C, Li Y. Interaction and nanotoxic effect of TiO_2 nanoparticle on fibrinogen by multi-spectroscopic method. Science of the Total Environment. 2012;429:156-160.

14. Kendall M, Ding P, Kendall K. Particle and nanoparticle interactions with fibrinogen: the importance of aggregation in nanotoxicology. Nanotoxicology. 2011;5:55-65.

15. Dalle-Donne I, Rossi R, Colombo R, Giustarini D, Milzani A. Biomarkers of oxidative damage in human disease. Clin. Chem. 2006;5:601-623.

16. Stadman E. Protein oxidation and aging. Free Radical Res. 2006;40:1250-1258.

17. Dalle-Donne I, Rossi R, Ceciliani F, Giustarini D, Colombo R, Milzani A. Proteins as sensitive biomarkers of human conditions associated with oxidative/nitrosative stress. In: Dalle-Donne I., Scaloni A, Butterfield D.A. (Eds.) Redox Proteomics: from Protein Modifications to Cellular Dysfunction and Diseases. Hoboken: John Wiley & Sons; 2006.

18. Roche M, Rondeau P, Sing NR, Tarnus E, Bourdon E. The antioxidant properties of serum albumin. FEBS Letters. 2008;582:1783-1787.

19. Tetik S, Kaya K, Demir M, Eksioglu-Demiralp E, Yardimi T. oxidative modification of fibrinogen affects its binding activity to glycoprotein (GP) IIb/IIIa. ThrombHemosClin Appl. 2010;16:51-59.

20. Weigandt KM, White N, Chung D, Ellingson E, Wang Y, Fu X, Pozzo DC. Fibrin clot structure and mechanics associated with specific oxidation of methionine residues in fibrinogen. Biophys J. 2012;103:2399-2407.

21. Lousinian S, Missopolinou D, Panayiotou C, Fibrinogen adsorption on zinc oxide nanoparticle: a micro-differential scanning calorimetry analysis. Journal of Colloid and Interface Sci. 2013;395:294-299.

22. Hawkins CL, Morgan PE, Davies MJ, Quantification of protein modification by oxidant. Free Radical Biology and Medicine. 2009;46(8):965-988.

23. Kandagal PB, Seetharamappa J, Ashoka S, Shaik SMT, Manjunatha DH. Study of the interaction between doxepin hydrochloride and bovine serum albumin by spectroscopic techniques. Int. J. Biol. Macromol. 2006;39:234-239.

24. Zhang YZ, Dai J, Zhang XP, Yang X, Liu Y, Studies of the interaction between sudan I and bovine serum albumin by spectroscopic methods. J. Mol. Struct. 2008;888:152-159.

25. Hu DH, Wu HM, Liang JG, Han HY. Study on the interaction between CdSe quantum dots and hemoglobin. Spectrochim. Acta A, 2008;69:830-834.

26. Zhenxing C, Rutao L. Phenotypic characterization of the binding of tetracycline to human serum albumin. Biomacromolecules. 2011;12:203-209.

27. Lacerda SH, Park JJ, Meuse C, Pristinski D, Becker ML, Karim A, Douglas JF. Interaction of gold nanoparticles with common human blood proteins. ACS NANO. 2010;4:365-379.

28. Yang Q, Liang J, Han H. Probing the interaction of magnetic iron oxide nanoparticles with bovine serum albumin by spectroscopic techniques. J. Phys. Chem. B. 2009;113:10454-10458.

29. Gharagozlou M, Boghaei DM. Interaction of water soluble amino acid Schiff base complexes with bovine serum albumin: fluorescence and circular dichroism studies. Spectrochim. Acta A. 2008;71(4):1617-1622.

30. Seetharamappa J, Kamat BP. Study of the interaction between fluoroquinolones and bovine serum albumin. J. Pharm. Biomed. Anal. 2005;39(5):1046-1050.

31. Yang P, Gao F. The Principles of Bioinorganic Chemistry. Science Press, Beijing; 2002.

32. Chong QJ, Ming XG, Ji XH. Study of the interaction between tetrazosin and serum albumin synchronous fluorescence determination. Anal. Chimica Acta. 2002;452:185-189.

33. Shahabadi N, Maghsudi M, Ahmadipour Z. Study on the interaction of Silver(I) complex with bovine serum albumin by spectroscopic techniques. SpectrochimicaActa Part A: Molecular and Biomolecular spectroscopy. 2012;92:184-188.

34. Shen XC, Liou XY, Ye LP, Liang H, Wang ZY. Spectroscopic studies between human hemoglobin CdS quantum dots. J. Colloid Interface Sci. 2007;311:400-406.

35. Yu CH, Al-saadi A, Shih SJ, Qui L, Tam KY, Tsang SC. Immobilization of BSA on silica coated magnetic iron oxide nanoparticle. J. Phys. Chem. C. 2009;113: 537-543.

36. Bulheller BM, Rodger A, Hirst JD. Circular and linear dichroism of proteins. Phys. Chem. Chem. Phys. 2007;9:2020-2035.

37. Carlisle CR, Coulais C, Namboothiry M, Carroll DL, Hantgan RR, Guthold M. The mechanical properties of individual electrospun fibrinogen fibers. Biomaterials. 2009; 30(6):1205-1213.

38. Tunc S, Maitz MF, Steiner G, Vazquez L, Pham MT, Salzer R. In situ conformational analysis of fibrinogen adsorbed on Si surfaces. Colloids and Surfaces B: Biointerfaces. 2005;42:219-222.

39. Yongoli C, Xiufang Z, Yandao G, Naming Z, Tingying Z, Xinqi S. Conformational changes of fibrinogen adsorption onto hydroxyapatite and titatiun oxide nanoparticles. Journal of Colloid and Interface Science. 1999; 214: 38-45.

40. Anraku M, Yamasaki K, Maruyama T, Kragh-Hansen U, Otagiri M. Effects of oxidative stress on the structure and function of human serum albumin. Pharmaceutical Research. 2001;18:632-639.

41. Petronio MS, Fernandes JR, Menezes ML, Ximenes VF. Oxidation of bovine albumin by hypoclorous and hypobromous acids: structural and functional alternations. British Journal of Pharmaceutical Research. 2013;3:147-160.

42. Malencik DA, Anderson SR. Dityrosine as product of oxidative stress and fluorescent probe. Amino Acids. 2003;25:233-247.